Published in final edited form as:
*Arterioscler Thromb Vasc Biol*. 2009 October ; 29(10): 1696–1701. doi:10.1161/ATVBAHA.109.192179.

# Hemorrhage and large lipid-rich necrotic cores are independently associated with thin or ruptured fibrous caps: An *In vivo* 3T MRI study

**Hideki Ota**[1,2], **Wei Yu**[3], **Hunter R. Underhill**[1], **Minako Oikawa**[1], **Li Dong**[1], **Xihai Zhao**[1], **Nayak L Polissar**[4], **Blazej Neradilek**[4], **Tianli Gao**[5], **Zhuo Zhang**[5], **Zixu Yan**[3], **Miao Guo**[3], **Zhaoqi Zhang**[3], **Thomas S. Hatsukami**[6], and **Chun Yuan**[1]

[1]Department of Radiology, University of Washington, Seattle, Washington

[2]Department of Radiology, Michigan State University, East Lansing, Michigan

[3]Department of Radiology, the Anzhen Hospital, Capital Medical University, Beijing China

[4]The Mountain-Whisper-Light Statistical Consulting, Seattle, Washington

[5]Department of Neurology, the Anzhen Hospital, Capital Medical University, Beijing China

[6]Department of Surgery, University of Washington, Seattle, Washington

## Abstract

**Objective—**Histological studies suggest associations between hemorrhage and large lipid-rich/necrotic cores with thin or ruptured fibrous caps in advanced atherosclerosis. We investigated these associations in carotid arteries with mild to severe stenosis by *in-vivo* 3T MRI.

**Methods and results—**Seventy-seven patients with ≥50% carotid stenosis in at least one side by duplex ultrasound underwent bilateral multi-contrast carotid MRI scans. Measurements for wall and lipid-rich/necrotic core sizes, presence of hemorrhage and fibrous cap status (classified as intact thick, intact thin or ruptured) were recorded. Arteries with poor image quality, occlusion or no detectable lipid-rich/necrotic core were excluded. For the 798 MRI slices included, multivariate ordinal regression analysis demonstrated larger %lipid-rich/necrotic core (odds ratio for 10% increase, 1.49; $p=0.02$) and presence of hemorrhage (odds ratio, 5.91; $p<0.001$) were independently associated with a worse (intact thin or ruptured) stage of fibrous cap status. For artery-based multivariate analysis, a larger maximum %lipid-rich/necrotic core and presence of hemorrhage independently associated with worse fibrous cap status ($p<0.001$, for both). No hemorrhage was detected in arteries with thick fibrous caps.

**Conclusion—**Hemorrhage and larger %lipid-rich/necrotic core were independently associated with a thin or ruptured fibrous cap status at an early to advanced stage of carotid atherosclerosis.

### Keywords

magnetic resonance imaging; carotid artery; fibrous cap rupture; hemorrhage; lipid-rich necrotic core

Correspondence: Chun Yuan, PhD, Address: Vascular Imaging Laboratory 815 Mercer St, Box 358050, Room 124, Seattle, WA 98109, Phone: 206.685.2231, Fax: 206.616.9346, cyuan@u.washington.edu.
**Equal contributions:** Hideki Ota and Wei Yu contributed equally to this work.

Atherosclerotic plaque rupture is the most frequent cause of arterial thrombosis, accounting for 60-65% of all coronary thrombi[1] and around 90% of thrombosed plaques from patients with stroke.[2]

Histological studies of coronary arteries have demonstrated that necrotic lipid cores are associated with plaque vulnerability, showing the mean value of percent necrotic core size is the greatest in ruptured plaque (34±17%), followed by thin-cap atheromas (23±17%) and fibrous cap atheromas (15±20%).[3-5] A recent histological study[6] of 50 whole hearts demonstrated an inverse relationship between necrotic core size and cap thickness; percentage of necrotic core size is significantly different between ruptured plaques (31.0±3.6%) and thick-capped fibroatheroma (17.2±1.8%) (p=0.0034). Intraplaque hemorrhage is also considered to contribute to plaque instability. Intraplaque hemorrhage shows associations with both an increase in the size of the necrotic core and lesion instability.[7]

The association of necrotic core size and hemorrhage with fibrous cap status has been also evaluated by studies of carotid endarterectomy specimens. A histological study of symptomatic patients demonstrated that presence of a thin cap is significantly associated with a large necrotic/lipid core.[8] Another study of 44 carotid endarterectomy specimens demonstrated that intraplaque hemorrhage correlates strongly with plaque rupture ($p<0.0001$).[9] Redgrave et al. [10] demonstrated in a histological assessment of 526 symptomatic carotid plaques that fibrous cap rupture showed strong positive associations with several other histology features, including: large lipid core (odds ratio [OR] 6.46, 95% confidence interval [CI] 4.37 to 9.55, $P<0.001$), hemorrhage (OR 4.38, 95% CI 2.98 to 6.42, $P<0.001$), and marked cap inflammation (OR 6.01, 95% CI 3.80 to 9.50, $P<0.001$). The histological assessment also showed that in a multivariate analysis, intraplaque hemorrhage and fibrous cap inflammation were independently associated with fibrous cap rupture.

These studies evaluated only advanced stages of atherosclerosis with severe stenosis following well-established treatment strategy,[11]. Little is known about the characteristics of carotid atherosclerosis in patients with early to moderate stenosis by histological studies. However, plaque rupture also occurs at low grade stenosis and the degree of stenosis poorly predicts events.[12] Therefore, it is important to evaluate a wide range of carotid atherosclerotic disease in order to understand the mechanism of plaque development and rupture.

*In vivo* carotid MRI has the ability to visualize atherosclerotic plaque components such as lipid-rich/necrotic core (LRNC), calcification, hemorrhage and fibrous cap, and has good concordance with histology.[13-19] Non-invasive imaging allows us to study plaque characteristics not only in advanced- but also early- to moderate-stage atherosclerosis, which holds potential to reveal the processes behind atherosclerosis progression.

The aim of this study was to investigate whether the size of LRNC and/or the presence of hemorrhage are associated with thin or ruptured fibrous caps in carotid arteries with mild to severe stenosis, using 3.0T MRI.

## Methods

This study was approved by the institutional review board and informed consent was obtained from all patients. Between February and September 2007, 77 consecutive patients hospitalized at the neurological department of Anzhen Hospital, Capital Medical University, Beijing, China were included: 33 patients were symptomatic and had acute ischemic stroke or transient ischemic attacks with ≥50% carotid stenosis in the ipsilateral side as measured by duplex ultrasound, and 44 were neurologically asymptomatic who sought treatment for their carotid artery diseases with ≥50% stenosis in at least one side. Patients were excluded prior to the carotid MR scan if there was: 1) a probable cardiac source of embolism, 2) Takayasu's arteritis,

3) intracranial artery stenosis proven by transcranial Doppler sonography and brain MR angiography, or 4) any contraindication for MRI. Symptomatic patients were imaged within 7 days after onset of symptoms. A total of 154 carotid arteries in 77 patients were included, this includes arteries with <50% stenosis on the less stenotic side.

### MRI protocol

Patients were imaged with a 3.0T whole body MR scanner (Signa Excite; General Electronic Healthcare, Waukesha, WI) and a phased-array carotid coil. The following five MR contrast weightings were obtained: three-dimensional time-of-flight (TOF), double inversion recovery pre-contrast T1-weighted (T1W) and gadolinium-based contrast-enhanced T1-weighted (CE-T1W), proton-density weighted (PDW), and T2-weighted (T2W). Gadopentetate dimeglumine (Magnevist; Bayer Schering Pharma AG, Berlin, Germany), 0.1 mmol/kg body weight, was injected intravenously to acquire CE-T1W images. Scan delay was 5 minutes after the injection based on previous reports to evaluate LRNC and fibrous cap validated by histology.[20,21] Scan protocols were as follows: for T1W and CE-T1W, repetition time/echo time/inversion time, 800/11/300ms; for PDW and T2W, repetition time, 3500ms, echo time 12.4/62.1ms; for TOF, repetition time/echo time 21/2.9ms, flip angle, 15°. All the images were obtained with field-of-view of 14.0*14.0 cm, matrix size of 256*256, slice thickness of 2mm. Inter-slice gaps were 2mm in T1W, T2W, PDW, and CE-T1W images, and 1mm in TOF images. Scan coverage was 3.2cm (32 slices) in TOF, and 3.4cm (17 slices) in other weightings. Scan coverage included the carotid artery bifurcation on both sides.

### MRI image review and criteria

Five trained reviewers, blinded to subject information, interpreted images. One reviewer evaluated all cases. The result was peer-reviewed by one of the other four reviewers. In cases where disagreement between the primary- and peer-review occurred, consensus agreement was reached after discussion.

Slice levels of all the image weightings were matched based on the level of extracranial carotid bifurcation. An image quality (IQ) score was assigned to each location by primary reviewers: IQ=1 indicated poor quality (arterial wall and lumen margins not identifiable); IQ=2, adequate quality (wall was visible, but the compositional substructure was partially obscured); IQ=3, good quality (minimal motion or flow artifacts, wall and lumen boundaries clearly defined); and IQ=4, excellent quality (no artifacts, wall architecture and plaque composition depicted in detail).[22] Imaging locations with an average IQ=1 were excluded from the image review.

At each location, area measurements of vessel wall and plaque components were measured using a computer-aided system for cardiovascular disease evaluation (CASCADE).[23] This program has been validated and has been used to evaluate carotid plaque for arteries with mild to severe stenosis.[24-27] Plaque features, including LRNC, calcification, and hemorrhage were determined according to previously published criteria,[13-16,20,24,25] based on relative tissue signal intensities compared to the adjacent muscle. In slices with LRNC, fibrous cap status (intact thick, intact thin or ruptured) was also evaluated[14,24,25,28] (Figures 1-3). Table 1 details the image interpretation criteria.

### Statistical analysis

Descriptive statistics are presented as means ± standard deviations (SD) for continuous variables and as numbers of cases and percentages per group for categorical variables.

For each slice the %LRNC was calculated as 100*LRNC area divided by wall area. Variables for artery-based analysis were the maximal value of %LRNC and the worst condition of fibrous cap status across all slices in an artery, as well as presence of hemorrhage. Slices or arteries

with no detectable LRNC or with a calcium nodule were excluded from the slice or artery analysis.

Univariate and multivariate ordinal logistic regression models were fitted to determine the association of hemorrhage and LRNC size with the fibrous cap status (ordered from best to worst as thick, thin and ruptured cap). The ordinal logistic regression models were fitted using generalized estimating equations (GEE) with exchangeable correlation structure in order to adjust for the correlation of the repeated measures within a patient. Separate models were fitted to the slice data and to the artery data. The multivariate models provided the adjusted odds ratios for fibrous cap status in relation to each of the two risk factors.

In the artery dataset, the logistic regression models for cap status with hemorrhage as an independent variable did not converge, due to the presence of a zero cell in the 2-by-3 crosstabulation of fibrous cap status vs. hemorrhage. (The zero cell indicated no hemorrhage in the thick cap group.) For these analyses, either stratified ordinal logistic regression or linear regression (estimated by GEE) was used.

Associations of symptoms with fibrous cap status and presence of clinical risk factors were also evaluated using logistic regression analysis, estimated with GEE. Variables with $p<0.2$ in the univariate model were considered for the multivariate analysis. Variables were selected into the final multivariate model using forward variable selection ($p<0.1$ for entry into model).

Computation was performed in R (Vienna, Austria), version 2.7.0. $P < 0.05$ was used to designate statistical significance.

## Results

Out of 154 arteries in 77 subjects, nine arteries were excluded before image matching (3 due to poor image quality across all slices, and 6 due to occlusion). In addition, 33 arteries with no detectable LRNC were excluded from statistical analysis. In the remaining 112 arteries (71 subjects), the mean ± SD of the degree of stenosis measured by duplex ultrasound was 51.5 ± 24.3% (range 0-99%). Table 2 shows baseline demographic data for the 71 subjects. Twenty-nine of the 71 patients had symptomatic arteries.

### Slice-based analysis

Out of 2329 slices in 145 arteries, 34 slices were excluded prior to image interpretation due to poor image qualities. Out of 2295 slices interpreted, 122 slices (5.3%) required mutual discussion for consensus agreement. The source of disagreement was from either low image quality or artifact that reduced certainty for image interpretation. After image interpretation, 1492 slices with no detectable LRNC and 5 with calcium nodules were excluded. Of the remaining 798 slices, 565 (71%) in 106 arteries had a thick cap, 194 (24%) in 65 arteries had a thin cap, and 39 (5%) in 16 arteries had a ruptured cap. Four patients had one slice with a ruptured cap, seven patients had two slices with a ruptured cap and five patients had 3-7 slices with a ruptured cap. The size of %LRNC and the number of slices with hemorrhage for each fibrous cap group are shown in Table 3.

Univariate ordinal logistic regression of the slice data showed a significant association of higher %LRNC with worse fibrous cap status (OR = 1.95 for every 10% increase in %LRNC; 95% CI, 1.53-2.47; $p<0.001$) and a significant increase in the risk of a worse fibrous cap status among those with vs. those without hemorrhage (OR =12.78; 95% CI, 8.33-19.61; $p<0.001$). Multivariate analysis found that both the presence of hemorrhage and larger %LRNC were independent risk factors for a worse stage of fibrous cap status. The odds ratios from the

multivariate model were OR = 1.49 for a 10% increment of %LRNC (95% CI, 1.04-2.13; p=0.02), and OR = 5.91 for presence vs. absence of hemorrhage (95% CI, 2.66-13.12; p<0.001).

### Artery-based analysis

Three arteries with calcium nodules were excluded. Of the remaining 109 arteries 43 (39%) were classified as thick, 50 (46%) as thin, and 16 (15%) as ruptured fibrous caps. The mean ± SD of maximal %LRNC and the number of arteries with hemorrhage for the individual groups are shown in Table 3. No hemorrhage was found in the thick fibrous cap group. Univariate ordinal logistic regression analysis found a significant association between maximal %LRNC and fibrous cap status (OR = 3.33 for a 10% increase in maximal %LRNC; 95% CI, 1.94-5.71; p<0.001). The odds ratio for this fibrous cap/%LRNC association, stratifying on hemorrhage presence or absence, was 1.83; 95% CI, 1.18-2.84, p = 0.003. The association of fibrous cap status with hemorrhage presence was highly significant in the univariate (p < 0.001) and multivariate linear regression analysis (p < 0.001, controlling for % LRNC). The “thin” and “ruptured” categories of fibrous cap status can be compared to obtain an OR in relation to presence or absence of a hemorrhage, yielding an unadjusted OR = 28 for a ruptured cap vs. a thin fibrous cap in relation to hemorrhage presence/absence (95% CI, 5-130, $p < 0.001$) and an adjusted OR = 17 (95% CI, 3-108, $p = 0.002$).

Univariate logistic regression analysis demonstrated that presence of diabetes and fibrous cap status were significantly associated with the presence of symptoms (OR=2.42, p=0.03 for presence vs. absence of diabetes; OR=1.90, $p$=0.04 for a change from thick to thin cap or from thin to ruptured cap, with the three levels of cap status coded as 0, 1, 2 for this analysis.) Among the other risk factors listed in Table 2, presence of coronary artery disease and hypercholesterolemia were also related to presence of symptoms, although these associations were not statistically significant (OR=1.86, $p$=0.19 and 2.15, $p$=0.06, respectively). All four variables were selected into the multivariate model, which demonstrated that fibrous cap status (OR=1.97, 95% CI, 1.02-3.80, $p$=0.04), as well as coronary artery disease (OR=3.67, 95% CI, 1.27-10.61, $p$=0.02), and diabetes (OR=2.61, 95% CI, 1.11-6.10, $p$=0.03) demonstrated a statistically significant independent association with symptom status; hypercholesterolemia (OR=2.28, 95% CI, 1.02-3.80, $p$=0.06) was marginally significant in the same model.

## Discussion

This study is based on *in vivo* imaging of carotid atherosclerosis with different levels of stenosis and thus various levels of clinical lesion stages. We showed that both %LRNC and presence of hemorrhage are associated with fibrous cap status and therefore plaque vulnerability. These two predictor variables have an independent effect on cap status—an effect consistent between the slice-based and artery-based analyses.

To understand the mechanism of fibrous cap destabilization is important because plaque rupture is the most frequent cause of arterial thrombosis. Previous *in vivo* MRI studies point to the mechanism of plaque progression and plaque features associated symptoms[28-31] However, none of those studies reported any association of plaque components qualitatively or quantitatively with fibrous cap status. The novelty of this study is that it is the first to reveal plaque features associated with thin or ruptured fibrous caps in carotid arteries with mild to severe stenosis. Furthermore, this study confirms that a thin or ruptured cap evaluated *in vivo* MRI was significantly associated with clinical symptoms. These results add to the understanding of mechanism of fibrous cap destabilization which results in thromboembolic events.

Fibrous cap is defined as a layer of connective tissue covering the LRNC.[5] Ruptured plaques have several histological features that are different from intact plaques: relatively large plaque

volumes, evidence of positive remodeling, large lipid cores, inflammatory cell infiltration, thin cap depleted of smooth muscle cells and collagen, and increased neovascularity.[32] The mechanism underlying the relationship between necrotic core size and fibrous cap status is not yet fully known.[6] Activated macrophages in necrotic cores secrete matrix metalloproteases and collagenases, which may retard the development of a thick, collagen-rich fibrous cap.[6] Those inflammatory cells are probably recruited into the atherosclerotic plaques by adhesion molecules and chemokines, or they may come into the plaques through the adventitial neovasculature.[32] Large LRNC may provide an environment where inflammatory cells can be activated. In addition, LRNC contains tissue factors which play important roles in promoting thrombosis when they are exposed to circulating blood.[33] The result that larger LRNC tends to have thin/ruptured fibrous caps also may indicate that a more severe catastrophic thromboembolic event would occur after the release of larger amount of thrombogenic materials.

Lin et al. demonstrated in an experiment using New Zealand white rabbits that injected erythrocytes in aortic plaques induced dose-dependently thinner fibrous cap, more macrophage infiltration, and more superoxide and lipid content.[34] Increased content of lipids and other pro-oxides derived from erythrocytes may promote inflammation in plaque, resulting in increased lipid content, recruitment of inflammatory cells and attenuated fibrous cap.[34] Our findings may lend support to their proposed mechanism of contribution of hemorrhage to fibrous cap destabilization.

The goal of slice-based analysis was to evaluate the morphological characteristics of carotid plaque in a manner comparable to histological cross-sectional evaluation.[3-6] On the other hand, the artery-based analysis was more clinically oriented. Yuan et al. demonstrated that identification of fibrous cap rupture by *in vivo* carotid MRI was highly associated with symptoms,[28] which was consistent with our result. Furthermore, no hemorrhage occurred in the thick fibrous cap group in our study. This may indicate that hemorrhage significantly affects plaque progression, making it more prone to rupture. Murphy et al.[30] demonstrated that the prevalence of hemorrhage/thrombus detected by *in vivo* MRI was higher in symptomatic carotids. Those arteries with hemorrhage have a high probability of fibrous cap ruptures.

One advantage of *in vivo* carotid MRI over histological studies is the ability to monitor atherosclerotic plaques at early to severe stages. Carotid endarterectomy studies offer clues to the mechanisms of plaque disruption but cannot document the process of plaque evolution.[9] The association of LNRC and hemorrhage with fibrous cap status in our study is consistent with previous histological studies regarding the course of development of atherosclerosis. Another advantage of *in vivo* MRI is the ability to perform longitudinal studies. Longitudinal clinical studies have demonstrated that the LRNC size decreases after statin treatment.[26,35] This study shows the ability of *in vivo* MRI to visualize features of the vulnerable plaque; a large necrotic core with thin cap. Further studies may capture subsequent fibrous cap rupture of vulnerable plaques, or reveal whether fibrous cap may regain thickness along with the regression of LRNC.

The measurement of LRNC relies mainly on the area of absent or limited enhancement on CE-T1W images compared with the surrounding, more strongly enhanced fibrous tissue.[15,20,21,24] It is reported that high enhancement is seen in area of neovasculature or loose extracellular matrix.[24,36] Although gadolinium may diffuse into the LRNC from such regions, it can be assumed that LRNC with little vasculature will enhance less than the surrounding tissue.

5.2% of interpreted slices needed mutual discussion for consensus agreement. This rate would be acceptable when compared to reported inter-reader reproducibility for *in vivo* carotid plaque

MRI (intra-class correlation coefficient = 0.73-0.95 for quantification [19,24,37,38], and weighted kappa = 0.83 for lesion type assessment.[39]

It is a limitation that our MRI protocols did not enable evaluation of the degree of inflammation which is likely to associate with fibrous cap rupture. Other studies suggest the potential of *in vivo* imaging of plaque inflammation using such as dynamic contrast MR imaging[36] and ultrasmall superparamagnetic iron oxide imaging.[40] With further development of the imaging protocol, multi-factorial analysis regarding fibrous cap status may help reveal the complex factors behind fibrous cap rupture further in addition to the present results.

In conclusion, large LRNC and presence of hemorrhage have a significant and independent association with a worse grade of fibrous cap status for carotid arteries with mild to severe carotid stenosis. These results reveal part of the process of atherosclerosis progression. Since fibrous cap rupture is considered a critical factor for subsequent thromboembolic events, the present results provide important information for the management of patients with carotid artery atherosclerosis.

## Acknowledgments

**Sources of Funding** This work was supported by the following NIH Grants: NIH R01-HL56874, NIH R01-HL073401, and NIH P01 HL072262

We thank Zach Miller for his help in preparing the manuscript.

## References

1. Virmani R, Burke AP, Kolodgie FD, Farb A. Pathology of the thin-cap fibroatheroma: a type of vulnerable plaque. Journal of Interventional Cardiology 2003;16:267–72. [PubMed: 12800406]
2. Spagnoli LG, Mauriello A, Sangiorgi G, Fratoni S, Bonanno E, Schwartz RS, Piepgras DG, Pistolese R, Ippoliti A, Holmes DR Jr. Extracranial thrombotically active carotid plaque as a risk factor for ischemic stroke. JAMA 2004;292:1845–52. [PubMed: 15494582]
3. Virmani R, Burke AP, Kolodgie FD, Farb A. Vulnerable plaque: the pathology of unstable coronary lesions. Journal of Interventional Cardiology 2002;15:439–46. [PubMed: 12476646]
4. Burke AP, Virmani R, Galis Z, Haudenschild CC, Muller JE. 34th Bethesda Conference: Task force #2--What is the pathologic basis for new atherosclerosis imaging techniques? J Am Coll Cardiol 2003;41:1874–86. [PubMed: 12798554]
5. Virmani R, Kolodgie FD, Burke AP, Farb A, Schwartz SM. Lessons from sudden coronary death: a comprehensive morphological classification scheme for atherosclerotic lesions. Arterioscler Thromb Vasc Biol 2000;20:1262–75. [PubMed: 10807742]
6. Cheruvu PK, Finn AV, Gardner C, Caplan J, Goldstein J, Stone GW, Virmani R, Muller JE. Frequency and distribution of thin-cap fibroatheroma and ruptured plaques in human coronary arteries: a pathologic study. J Am Coll Cardiol 2007;50:940–9. [PubMed: 17765120]
7. Kolodgie FD, Gold HK, Burke AP, Fowler DR, Kruth HS, Weber DK, Farb A, Guerrero LJ, Hayase M, Kutys R, Narula J, Finn AV, Virmani R. Intraplaque hemorrhage and progression of coronary atheroma. N Engl J Med 2003;349:2316–25. [PubMed: 14668457]
8. Lammie GA, Wardlaw J, Allan P, Ruckley CV, Peek R, Signorini DF. What pathological components indicate carotid atheroma activity and can these be identified reliably using ultrasound? European Journal of Ultrasound: Official Journal of the European Federation of Societies for Ultrasound in Medicine and Biology 2000;11:77–86. [PubMed: 10781655]
9. Carr S, Farb A, Pearce WH, Virmani R, Yao JS. Atherosclerotic plaque rupture in symptomatic carotid artery stenosis. J Vasc Surg 1996;23:755–65. [PubMed: 8667496]discussion 765-6
10. Redgrave JNE, Lovett JK, Gallagher PJ, Rothwell PM. Histological assessment of 526 symptomatic carotid plaques in relation to the nature and timing of ischemic symptoms: the Oxford plaque study. Circulation 2006;113:2320–8. [PubMed: 16651471]

11. Beneficial effect of carotid endarterectomy in symptomatic patients with high-grade carotid stenosis. North American Symptomatic Carotid Endarterectomy Trial Collaborators. N Engl J Med 1991;325:445–53. [PubMed: 1852179]
12. Wasserman BA, Wityk RJ, Trout HH, Virmani R. Low-grade carotid stenosis: looking beyond the lumen with MRI. Stroke 2005;36:2504–13. [PubMed: 16239630]
13. Yuan C, Mitsumori LM, Ferguson MS, Polissar NL, Echelard D, Ortiz G, Small R, Davies JW, Kerwin WS, Hatsukami TS. In vivo accuracy of multispectral magnetic resonance imaging for identifying lipid-rich necrotic cores and intraplaque hemorrhage in advanced human carotid plaques. Circulation 2001;104:2051–6. [PubMed: 11673345]
14. Hatsukami TS, Ross R, Polissar NL, Yuan C. Visualization of fibrous cap thickness and rupture in human atherosclerotic carotid plaque in vivo with high-resolution magnetic resonance imaging. Circulation 2000;102:959–64. [PubMed: 10961958]
15. Yuan C, Kerwin WS, Ferguson MS, Polissar N, Zhang S, Cai J, Hatsukami TS. Contrast-enhanced high resolution MRI for atherosclerotic carotid artery tissue characterization. J Magn Reson Imaging 2002;15:62–7. [PubMed: 11793458]
16. Cai JM, Hatsukami TS, Ferguson MS, Small R, Polissar NL, Yuan C. Classification of human carotid atherosclerotic lesions with in vivo multicontrast magnetic resonance imaging. Circulation 2002;106:1368–73. [PubMed: 12221054]
17. Toussaint JF, LaMuraglia GM, Southern JF, Fuster V, Kantor HL. Magnetic resonance images lipid, fibrous, calcified, hemorrhagic, and thrombotic components of human atherosclerosis in vivo. Circulation 1996;94:932–8. [PubMed: 8790028]
18. Clarke SE, Hammond RR, Mitchell JR, Rutt BK. Quantitative assessment of carotid plaque composition using multicontrast MRI and registered histology. Magn Reson Med 2003;50:1199–208. [PubMed: 14648567]
19. Trivedi RA, U-King-Im JM, Graves MJ, Horsley J, Goddard M, Kirkpatrick PJ, Gillard JH. MRI-derived measurements of fibrous-cap and lipid-core thickness: the potential for identifying vulnerable carotid plaques in vivo. Neuroradiology 2004;46:738–43. [PubMed: 15309350]
20. Wasserman BA, Smith WI, Trout HH 3rd, Cannon RO 3rd, Balaban RS, Arai AE. Carotid artery atherosclerosis: in vivo morphologic characterization with gadolinium-enhanced double-oblique MR imaging initial results. Radiology 2002;223:566–73. [PubMed: 11997569]
21. Kramer CM, Cerilli LA, Hagspiel K, DiMaria JM, Epstein FH, Kern JA. Magnetic resonance imaging identifies the fibrous cap in atherosclerotic abdominal aortic aneurysm. Circulation 2004;109:1016–21. [PubMed: 14967731]
22. Underhill HR, Yarnykh VL, Hatsukami TS, Wang J, Balu N, Hayes CE, Oikawa M, Yu W, Xu D, Chu B, Wyman BT, Polissar NL, Yuan C. Carotid plaque morphology and composition: initial comparison between 1.5- and 3.0-T magnetic field strengths. Radiology 2008;248:550–60. [PubMed: 18574135]
23. Kerwin W, Xu D, Liu F, Saam T, Underhill H, Takaya N, Chu B, Hatsukami T, Yuan C. Magnetic resonance imaging of carotid atherosclerosis: plaque analysis. Top Magn Reson Imaging 2007;18:371–8. [PubMed: 18025991]
24. Cai J, Hatsukami TS, Ferguson MS, Kerwin WS, Saam T, Chu B, Takaya N, Polissar NL, Yuan C. In vivo quantitative measurement of intact fibrous cap and lipid-rich necrotic core size in atherosclerotic carotid plaque: comparison of high-resolution, contrast-enhanced magnetic resonance imaging and histology. Circulation 2005;112:3437–44. [PubMed: 16301346]
25. Saam T, Cai J, Ma L, Cai YQ, Ferguson MS, Polissar NL, Hatsukami TS, Yuan C. Comparison of symptomatic and asymptomatic atherosclerotic carotid plaque features with in vivo MR imaging. Radiology 2006;240:464–72. [PubMed: 16864672]
26. Underhill HR, Yuan C, Zhao XQ, Kraiss LW, Parker DL, Saam T, Chu B, Takaya N, Liu F, Polissar NL, Neradilek B, Raichlen JS, Cain VA, Waterton JC, Hamar W, Hatsukami TS. Effect of rosuvastatin therapy on carotid plaque morphology and composition in moderately hypercholesterolemic patients: a high-resolution magnetic resonance imaging trial. Am Heart J 2008;155:584.e1–8. [PubMed: 18294500]
27. Saam T, Underhill HR, Chu B, Takaya N, Cai J, Polissar NL, Yuan C, Hatsukami TS. Prevalence of American Heart Association type VI carotid atherosclerotic lesions identified by magnetic resonance

imaging for different levels of stenosis as measured by duplex ultrasound. J Am Coll Cardiol 2008;51:1014–21. [PubMed: 18325441]

28. Yuan C, Zhang SX, Polissar NL, Echelard D, Ortiz G, Davis JW, Ellington E, Ferguson MS, Hatsukami TS. Identification of fibrous cap rupture with magnetic resonance imaging is highly associated with recent transient ischemic attack or stroke. Circulation 2002;105:181–5. [PubMed: 11790698]
29. Takaya N, Yuan C, Chu B, Saam T, Polissar NL, Jarvik GP, Isaac C, McDonough J, Natiello C, Small R, Ferguson MS, Hatsukami TS. Presence of intraplaque hemorrhage stimulates progression of carotid atherosclerotic plaques: a high-resolution magnetic resonance imaging study. Circulation 2005;111:2768–75. [PubMed: 15911695]
30. Murphy RE, Moody AR, Morgan PS, Martel AL, Delay GS, Allder S, MacSweeney ST, Tennant WG, Gladman J, Lowe J, Hunt BJ. Prevalence of complicated carotid atheroma as detected by magnetic resonance direct thrombus imaging in patients with suspected carotid artery stenosis and previous acute cerebral ischemia. Circulation 2003;107:3053–8. [PubMed: 12796136]
31. Takaya N, Yuan C, Chu B, Saam T, Underhill H, Cai J, Tran N, Polissar NL, Isaac C, Ferguson MS, Garden GA, Cramer SC, Maravilla KR, Hashimoto B, Hatsukami TS. Association between carotid plaque characteristics and subsequent ischemic cerebrovascular events: a prospective assessment with MRI--initial results. Stroke 2006;37:818–23. [PubMed: 16469957]
32. Shah PK. Mechanisms of plaque vulnerability and rupture. J Am Coll Cardiol 2003;41:15S–22S. [PubMed: 12644336]
33. Dickson BC, Gotlieb AI. Towards understanding acute destabilization of vulnerable atherosclerotic plaques. Cardiovasc Pathol 12:237–48. [PubMed: 14507572]
34. Lin HL, Xu XS, Lu HX, Zhang L, Li CJ, Tang MX, Sun HW, Liu Y, Zhang Y. Pathological mechanisms and dose dependency of erythrocyte-induced vulnerability of atherosclerotic plaques. J Mol Cell Cardiol 2007;43:272–80. [PubMed: 17628589]
35. Corti R, Fuster V, Fayad ZA, Worthley SG, Helft G, Smith D, Weinberger J, Wentzel J, Mizsei G, Mercuri M, Badimon JJ. Lipid lowering by simvastatin induces regression of human atherosclerotic lesions: two years' follow-up by high-resolution noninvasive magnetic resonance imaging. Circulation 2002;106:2884–7. [PubMed: 12460866]
36. Kerwin WS, O'Brien KD, Ferguson MS, Polissar N, Hatsukami TS, Yuan C. Inflammation in carotid atherosclerotic plaque: a dynamic contrast-enhanced MR imaging study. Radiology 2006;241:459–468. [PubMed: 16966482]
37. Cappendijk VC, Heeneman S, Kessels AG, Cleutjens KB, Schurink GW, Welten RJ, Mess WH, van Suylen RJ, Leiner T, Daemen MJ, van Engelshoven JM, Kooi ME. Comparison of single-sequence T1w TFE MRI with multisequence MRI for the quantification of lipid-rich necrotic core in atherosclerotic plaque. J Magn Reson Imaging 2008;27:1347–1355. [PubMed: 18504754]
38. Saam T, Ferguson MS, Yarnykh VL, Takaya N, Xu D, Polissar NL, Hatsukami TS, Yuan C. Quantitative evaluation of carotid plaque composition by in vivo MRI. Arterioscler Thromb Vasc Biol 2005;25:234–9. [PubMed: 15528475]
39. Chu B, Phan BA, Balu N, Yuan C, Brown BG, Zhao XQ. Reproducibility of carotid atherosclerotic lesion type characterization using high resolution multicontrast weighted cardiovascular magnetic resonance. J Cardiovasc Magn Reson 2006;8:793–799. [PubMed: 17060101]
40. Howarth SP, Tang TY, Trivedi R, Weerakkody R, U-King-Im J, Gaunt ME, Boyle JR, Li ZY, Miller SR, Graves MJ, Gillard JH. Utility of USPIO-enhanced MR imaging to identify inflammation and the fibrous cap: A comparison of symptomatic and asymptomatic individuals. European Journal of Radiology. in press

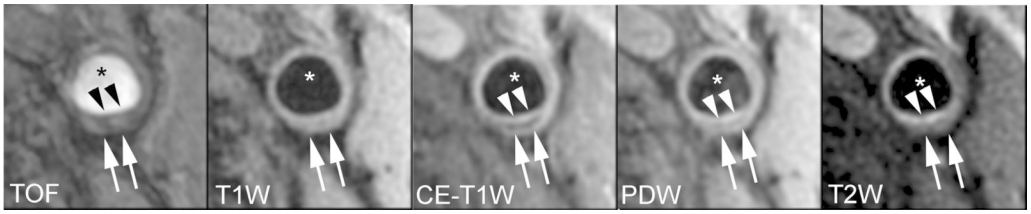


**Figure 1.**
Lipid-rich/necrotic core (arrows) with overlying intact thick fibrous cap. A smooth luminal surface and visible juxtaluminal band on TOF, CE-T1W, PDW, and T2W images indicate intact thick fibrous cap (arrow heads). * indicates lumen.

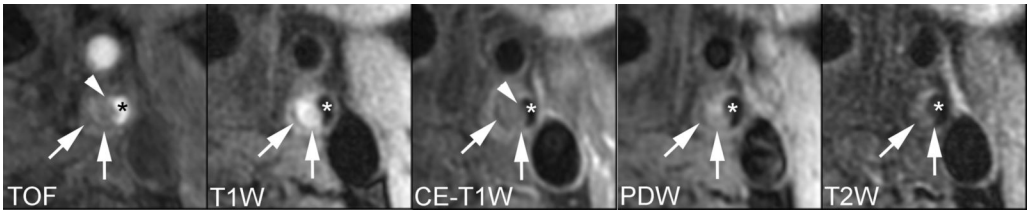


**Figure 2.**
Lipid-rich/necrotic core (arrows) with overlying intact thin fibrous cap. Smooth surface with juxtaluminal band not apparent on TOF, CE-T1W, PDW, and T2W images indicates intact thin fibrous cap (arrow heads). * indicates lumen.

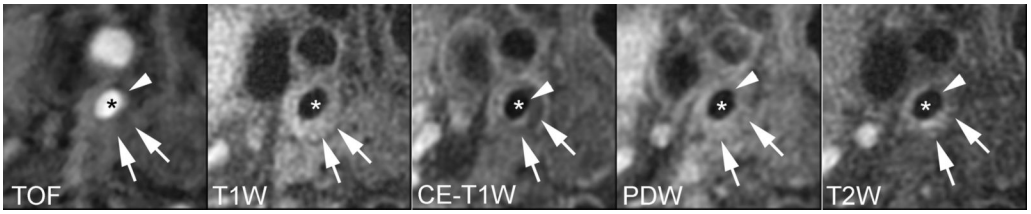


**Figure 3.**

Hemorrhagic lipid-rich/necrotic core (arrows) with ruptured fibrous cap. Area with hypointensity on CE-T1W and hyperintensity on other images indicates a hemorrhagic lipid-rich/necrotic core. A surface irregularity of the lumen, a hyperintense juxtaluminal signal on TOF and invisible juxaluminal band on CE-T1W indicate ruptured fibrous cap (arrow heads). * indicates lumen.

**Table 1**

Image Interpretation criteria

| | TOF | T1W | PDW | T2W | CE-T1W |
|---|---|---|---|---|---|
| LRNC with no hemorrhage | ○ | ○/+ | ○/+ | -/○ | - |
| Intraplaque hemorrhage | + | + | variable* | variable* | - |
| Intact thick | Smooth surface on all images with juxtaluminal band between LRNC and lumen on CE-T1W. | | | | |
| Intact thin | Smooth surface on all images and juxtaluminal band not apparent on CE-T1W. | | | | |
| Ruptured | Irregular surface on all images and a hyperintense signal adjacent to the lumen on TOF and invisible juxtaluminal band on CE-T1W. | | | | |

The classification of LRNC and hemorrhage is based on the following signal intensity relative to adjacent muscle: +, hyperintense; ○, isointense; -, hypointense.

*Signal intensities are variable due to the hemorrhage type.

**Table 2**

Baseline demographic data for 71 patients.

| Characteristic or Risk Factor | Mean ± SD or % |
|---|---|
| Age, years (range) | 67.2 ± 9.7 (44-86) |
| Male sex, % | 75 |
| Height, meters | 1.67 ± 0.07 |
| Weight, kg | 70.6 ± 11.3 |
| Body mass index, $kg/m^2$ | 25.2 ± 3.6 |
| Hypertension, % | 72 |
| Hypercholesterolemia, % | 34 |
| Diabetes, % | 37 |
| Smoking, % | 56 |
| History of coronary artery disease, % | 17 |
| Symptom, % | 41 |

**Table 3**

Associations among LRNC size, presence of hemorrhage, and fibrous cap status. Ordinal logistic regression was used for the univariate and multivariate models, unless otherwise specified.

| | Fibrous cap status | | | Univariate model | | Multivariate model | |
|---|---|---|---|---|---|---|---|
| | **Thick** | **Thin** | **Ruptured** | **OR (95%CI)** | **p** | **OR (95%CI)** | **p** |
| **Slice based** | | | | | | | |
| N | 565 | 194 | 39 | | | | |
| Hemorrhage present (%) | 27 (5) | 54(28) | 25(64) | 12.78 (8.33-19.61) | <0.001 | 5.91 (2.66-13.12) | <0.001 |
| %LRNC (OR: per 10%) | 20.1 ±11.8* | 33.4 ±15.0* | 41.3 ±19.3* | 1.95 (1.53-2.47) | <0.001 | 1.49 (1.04-2.13) | 0.02 |
| **Artery based** | | | | | | | |
| N | 43 | 50 | 16 | | | | |
| Hemorrhage present (%) | 0 (0) | 10(20) | 14(88) | NA† | <0.001‡ | NA† | <0.001‡ |
| Maximum %LRNC (OR: per 10%) | 22.5 ±11.0* | 39.4 ±12.2* | 53.1±13.8* | 3.33 (1.94-5.71) | <0.001 | 1.83 (1.18-2.84) § | 0.003§ |

*Mean ± SD;

†OR cannot be computed for 3-level cap status variable from ordinal logistic regression; for ruptured vs. thin cap unadjusted OR = 28 (95% CI, 5-130, p < 0.001), adjusted OR = 17 (95% CI, 3-108, p = 0.002).

‡p-value from linear regression analysis;

§ordinal logistic regression stratified on hemorrhage presence/absence.